Journal of the European Ceramic Society 20 (2000) 1815–1828

# Transformation and thermal stability of Li-α-sialon ceramics

Z.B. Yu [a], D.P. Thompson [a,*], A.R. Bhatti [b]

[a] *Materials Division, Department of Mechanical, Materials and Manufacturing Engineering, University of Newcastle, Newcastle upon Tyne NE1 7RU, UK*
[b] *Structural Materials Centre, DERA Farnborough, Hampshire GU14 0LX, UK*

Received 14 September 1999; accepted 3 January 2000

**Abstract**

Two phase α/β and single phase α lithium sialons with different *m* and *n* values were produced by hot pressing at 1730–1750°C at 30 MPa for 30–40 min in a graphite resistance furnace. When the two-phase samples were heat-treated at lower (1200–1450°C) temperatures in different packing powders, an increase in the amount of α was observed, due to β-sialon in the as-sintered material reacting with grain boundary liquid to form more α. β→α transformation at low temperatures has not been reported previously in any sialon system and in the present case is believed to occur because the α-sialon phase field in the lithium sialon system shifts slightly towards the β-sialon line at lower temperatures. The thermal stability of lithium α-sialon is good in the centre of the single-phase α region when surrounded by a Li-containing powder bed. However, towards the edges of the single-phase region, compositional changes occur on heat-treatment. Thus, samples with high *m*, *n* values decompose into β-sialon plus other Li-containing phases. During heat-treatment of other compositions when surrounded by a BN powder bed, the composition of the α-sialon phase continually readjusts towards the α/β sialon phase region as a function of time and this is followed by decomposition of the α phase. Evaporation of the $Li^+$ stabilising cation is believed to be the main reason for this behaviour. The effects of *m* and *n* value, heat treatment parameters and packing powder on the thermal stability of Li α-sialons are discussed. 

*Keywords:* Annealing; Lithium sialon; Phase equilibria; Sialons; Thermal stability

## 1. Introduction

α- And β-sialons are solid solutions of aluminium and oxygen in α- and β-$Si_3N_4$ with formulae of the type $M_x Si_{12-(m+n)} Al_{(m+n)} O_n N_{16-n}$, and $Si_{6-z}Al_zO_zN_{8-z}$, respectively. In α-sialon, $(m+n)$ Si–N bonds in α-$Si_3N_4$ are replaced by *m* (Al–N) bonds and *n* (Al–O) bonds, the charge discrepancy being compensated for by cations M (typically Li, Mg, Ca, Y and Ln with $Z=58$) occupying the interstices in the (Si, Al)–(O, N) network. α′ Can therefore be regarded as a substitutional/interstitial solid solution phase. In β-sialon, where *z* (Al–O) bonds replace *z* (Si–N) bonds, the behaviour is purely substitutional. Therefore, it is accepted that because α- and β-sialons have different compositions and crystal structures, transformations between them are actually chemical reactions rather than polymorphic transformations and can be expressed by equations[1,2] such as:

$$\alpha - \text{sialon} + \text{oxides} \rightarrow \beta - \text{sialon} + \text{glass} \quad (1)$$

$$\beta - \text{sialon} + \text{nitrides} \rightarrow \alpha - \text{sialon} \quad (2)$$

The observation of α or β as the thermodynamically stable phase is determined by phase relationships in the appropriate M–Si–Al–O–N system.

It is well established that whereas in the case of silicon nitride, α→β transformation proceeds above 1400° C in the presence of a suitable liquid to lower the activation energy, and β→α transformation has not been observed under any conditions, in sialon systems, various authors (see for example Mandal et al.[3] and Thompson[4]) have shown that many rare earth densified α/β sialon compositions can undergo in-situ, reversible, α↔β-sialon transformation without further addition of oxides or nitrides, by heat treatment at temperatures below the sintering temperature. Since α- and β-sialons have different mechanical properties (i.e. α has the higher hardness and β the better strength and fracture toughness), this discovery of α↔β transformation provides a reliable

* Corresponding author.
*E-mail address:* d.p.thompson@ncl.ac.uk (D.P. Thompson).

0955-2219/00/$ - see front matter 
PII: S0955-2219(00)00044-3

method for tailoring the microstructure and hence the properties of α/β-sialon composites. From these previous studies, two important points emerge relating to the direction of the transformation and the reaction mechanism:

Firstly, yttrium and rare-earth stabilised α-sialons (see, for example[3,5]) are generally stable at high temperatures and transformation to β occurs at lower temperatures (1000–1500°C). Thus, for example, Shen et al.[6–10] reported a Nd–α-sialon phase to be unstable below 1650°C and a Yb–α-sialon which transformed to β at 1450°C. Zhao et al.[11,12] found that in the Sm–α-sialon system, α↔β phase transformation also occurred below 1450°C. In contrast, Hewett et al.[13,14] reported that α→β phase transformation occurred in Ca α-sialons, but only after heat-treatment at 1450°C for very long times (720 h). It is now accepted that apart from certain high-Z rare earth α-sialon compositions which are very stable, the transformation between α and β is fully reversible in Y and Ln α-sialon systems. Consistent with this, transformation from β to α in α/β-sialon ceramics has never been reported at low temperatures.

As regards the mechanism of transformation, extensive research in the Ca-, Y- and Ln-sialon systems based on a variety of α-sialon compositions, has shown different types of transformation behaviour with different reasons for the transformation, as a result of which both the thermal stability of α-sialon and the mechanism of α→β sialon transformation are still not fully understood.

Obviously the collection of more experimental data in other M–Si–Al–O–N systems is helpful in this respect and it is also important to explore variations in behaviour in these systems as a function of composition. In the present study therefore, a series of single-phase and two-phase α/β lithium sialons with systematically varying $m$ and $n$ values has been prepared and heat treated under different conditions to evaluate the thermal stability of the α phase as a function of composition and to obtain more information about the α⟺β transformation mechanism. Compositions have been selected as follows:

$m = 0.5$ Series. This series was designed to examine whether α→β transformation could take place easily at low heat-treatment temperatures, since the β sialon grains remaining after sintering act as nucleation sites.

$m = 1.0$ Series. This series was designed to study α→β transformation in single-phase α-sialon compositions close to the boundary with the α/β two-phase region; different $n$ values were used to examine the effect of oxygen/nitrogen ratio on thermal stability and transformation.

$1.0 < m < 2.0$ Series. These compositions were located within the single phase α-sialon region and were expected to be more stable with respect to transformation than the $m = 1.0$ series.

$m = 2.0$ Series. These samples contained the largest amount of stabilising cation which could be incorporated into the α-sialon structure. The samples were designed to examine the effect of time on α→β transformation, since it has been claimed that the stability of the α-sialon structure increases with increasing concentration of the stabilising cation.

## 2. Experimental procedures

Compositions were selected on the α-sialon plane of the Li–Si–Al–O–N phase diagram with reference to phase relationships previously determined[15] as shown in Fig. 1.

Starting powders (α-$Si_3N_4$, H. C. Starck, Grade G11; $Al_2O_3$, Alcoa; AlN H. C. Starck, Grade B; $Li_2CO_3$, BDH 99%; $SiO_2$, BDH precipitated) were mixed in appropriate proportions to achieve the desired compositions, taking into account the residual oxygen content of $Si_3N_4$ and AlN. The powder mixes in batches of 30 g were milled in isopropanol for 12 h using sialon milling media in a rubber-lined cylinder. The slurry was subsequently dried under an infra-red lamp while being stirred.

Four grams of as-mixed powder was initially cold-pressed into green-body compacts and then hot-pressed for 30–40 min at 1730–1750°C under 30 MPa pressure in a graphite die. After completion of densification, the furnace was shut down to allow rapid cooling at a cooling rate of 50°C/min. The sintered samples were heat-treated at temperatures between 1200 and 1450°C for 168, 336 and 500 h in an alumina tube furnace in a nitrogen atmosphere. Both BN- and Li-containing powders were used to surround the sample during this heat treatment.

Analysis of the crystalline phases present in the samples was based on their x-ray diffraction patterns obtained using a Guinier–Hägg focusing camera with Cu$K_{\alpha 1}$ radiation. Crystalline Si powder was used as the internal standard. The photographs obtained were analysed with a computer-linked SCANPI system and the cell parameters were determined with the program PIRUM. The amounts of α and β sialon phases were calculated by quantitative estimation from XRD patterns using the integrated intensities of the (102) and (210) reflections of

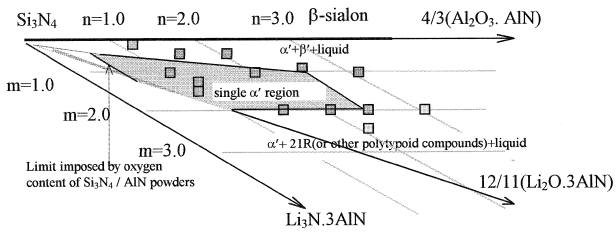


Fig. 1. Single phase α-sialon region in the Li–α-sialon plane (after[15]). Squares indicate the compositions investigated.

α-sialon and the (101) and (210) reflections of β-sialon in the following equation:

$$I_\beta/(I_\alpha + I_\beta) = 1/\{1 + K[(1/W_\beta) - 1]\}$$

where $I_\alpha$ and $I_\beta$ are the observed intensities of α- and β-sialon lines, respectively. $W_\beta$ is the relative weight fraction of β-sialon, $K$ ($=K_\alpha/K_\beta$) is the combined proportionality constant resulting from the constants in the two equations, namely:

$$I_\beta = K_\beta \times W_\beta$$
$$I_\alpha = K_\alpha \times W_\alpha$$

which is 0.518 for $\beta_{(101)}$–$\alpha_{(102)}$ reflections and 0.544 for $\beta_{(210)}$–$\alpha_{(210)}$ reflections.[16]

$z$-Values of β-sialons were obtained from the average of $z_a$ and $z_c$ given by:[4]

$$z_a = (\mathbf{a} - 7.6044)/0.03053$$

$$z_c = (\mathbf{c} - 2.9075)/0.02618$$

where **a** and **c** are the observed unit cell dimensions of β-sialon.

A Hitachi S-2400 scanning electron microscope was used for phase identification and microstructural characterisation. Specimens for scanning electron microscopy (SEM) examination were polished and etched in hot molten KOH to reveal their microstructures.

## 3. Results

### 3.1. Heat-treatment at 1200°C

#### 3.1.1. Two phase α/β-sialon compositions

*3.1.1.1. (a) In Li-containing packing powder*. In order to examine whether α↔β phase transformation occurred in Li–α-sialons in the same way as in rare earth stabilised α-sialons, it was important to avoid volatilisation of lithium which might automatically promote α→β transformation. Selected samples (compositions are given in Table 1) were therefore initially heat-treated at low temperatures (1200°C) using a Li-containing packing powder.

For two phase α/β-sialons, changes in α:β ratio could be clearly seen from their X-ray diffractometry (XRD) patterns (see Fig. 2). The relative amounts and unit cell dimensions of the α- and β-phases before and after heat-treatment at 1200°C in the presence of the Li-containing packing powder are shown in Tables 1 and 2.

In some rare-earth systems, pure α-sialons which are thermodynamically unstable will spontaneously transform into β-sialon when heat treated at lower temperatures; in other systems, the presence of β-sialon nuclei makes the transformation much easier. However, from Fig. 2 and Table 1, it is clear that in two-phase Li α/β-compositions, transformation did occur, but the transformation direction at 1200°C was from β→α instead of α→β. For example, the $m=0.5$, $n=1.5$ sample, which contained 81.8% α and 18.2% β after sintering, changed to 99% α and 1% β after heat-treatment for 168 h at 1200°C surrounded by a Li-containing packing powder, whilst the $m=0.5$, $n=2.0$ sample changed from 41% α, 59% β to 79% α, 21% β; moreover, the $m=1.0$, $n=3.0$ composition, which contained 12.4% β after sintering, completely transformed to α-sialon after heat treatment. These changes can be clearly seen from their XRD patterns (Fig. 2). The β→α-sialon transformation was previously believed to occur by chemical reactions such as :

$$\mathrm{Si_{6-z}Al_zO_zN_{8-z}} + \text{lithium-nitride} \rightarrow \mathrm{Li_xSi_{12-(m+n)}Al_{(m+n)}O_nN_{16-n}} \quad (3)$$

but in the present work, it must occur either because β-sialon reacts with crystalline or vitreous Li–Si–Al–O–N grain boundary material or because β-sialon has reacted with Li- and N-containing materials in the packing powder either by direct contact or through vapour diffusion. This point is discussed in more detail in the next section.

*3.1.1.2. (b) In BN packing powder*. The same samples were heat treated at the same temperature (1200°C) for the same time (168 h), but surrounded by pure BN packing powder. The heat-treatment results at 1200°C for 168 h in BN packing powder are given in Table 1 and Fig. 2.

Table 1 indicates that β→α transformation also occurred when BN packing powder was used instead of Li-containing packing powder, suggesting that the transformation is taking place in-situ and is not being assisted by Li-containing species present in the packing powder. This can be clearly seen from Fig. 2. However, it is worth noting that the amount of transformation is different (Fig. 3) when the alternative packing powder was used.

Fig. 3 shows that the type of packing powder has an effect on β→α transformation with apparently Li-containing packing powder having more effect on the $m=0.5$, $n=1.5$ and $m=0.5$, $n=2.0$ samples than on the $m=1.0$, $n=3.0$ sample. As can be seen from Fig. 3, more transformation occurred in the first two samples when Li-containing packing powder was used. This phenomenon can be understood if the phase changes before and after heat-treatment are taken into account. From Table 1, it can be seen that very small amounts of a second phase denoted here as β–LiSiON(Al) (an Al- and Li-substituted $Si_2N_2O$ phase[17]) were present in the

Table 1
Phase changes before (HP) and after heat-treatment (HT) at low (1200–1450°C) temperatures

| Composition ($m$, $n$) | As HP | | 1200°C/168 h (Li) | | 1200°C/168 h (BN ) | | 1200°C/336 h (BN) | | 1300°C/168 h (BN) | | 1300°C/500 h (BN) | | 1450°C/168 h (BN) | |
|---|---|---|---|---|---|---|---|---|---|---|---|---|---|---|
| | α′/β′ | Other phases[a] | α′/β′ | Other phases[a] | α′/β′ | Other phases[a] | α′/β′ | Other phases[a] | α′/β′ | Other phases[a] | α′/β′ | Other phases[a] | α′/β′ | Other phases[a] |
| (0.5, 1.5) | 83/17 | SN (vw) | 99/1 | – | 86/14 | – | 96/4 | SN? | 86/14 | SN? | 88/12 | SN? | 90/10 | SN |
| (0.5, 2.0) | 41/59 | SN (vw) | 79/21 | – | 66/34 | – | 70/30 | SN? | 65/35 | SN? | 58/42 | SN? | 55/45 | SN |
| (1.0, 1.0) | 100/0 | Eu (vw) | 100/0 | – | 100/0 | O′ | 100/0 | SN? | 100/0 | SN? | 100/0 | SN? | 100/0 | SN |
| (1.0, 2.0) | 100/0 | Eu (vw) | 100/0 | – | 100/0 | O′ | 100/0 | – | 100/0 | – | 98/2 | SN? | 84/16 | SN |
| (1.0, 2.5) | 100/0 | 12H (vw) | 100/0 | 12H | 100/0 | O′ | 100/0 | 12H | 100/0 | – | 96/4 | 12H? | 92/8 | – |
| (1.0, 3.0) | 88/12 | | 100/0 | O′[b] | 100/0 | O′ | 100/0 | – | 100/0 | – | 96/4 | 12H? | 89/11 | 15R |
| (1.3, 1.2) | 100/0 | Eu (vw) | –/– | – | 100/0 | | –/– | – | –/– | – | –/– | – | 100/0 | O′ |
| (1.5, 1.5) | 100/0 | Eu (vw) | | | 100/0 | | –/– | – | –/– | – | 97/3 | O′ 12H? | 100/0 | O′ |
| (2.0, 2.0) | 100/0 | Eu,21R (w) | 100/0 | | 100/0 | O′ | 100/0 | O′,12H | 100/0 | O′(m) | 86/14 | 12H? | 93/7 | 15R |
| (2.0, 2.5) | 100/0 | 21R (vw) | 100/0 | | 100/0 | O′, 21R | 100/0 | O′, 12H | 100/0 | 12H? | 78/22 | 12H? | 92/8 | 15R(m) |
| (2.0, 3.0) | | Eu,21R (m) | 100/0 | | 100/0 | O′, 21R | 100/0 | O′, 12H, 21R | 100/0 | O′(m) 12H? | 78/22 | 12H? | 81/19 | 15R(m) |

[a] X-ray peak intensity: vw = very weak, m = medium, s = strong.
[b] O′ = β-LiSiON(Al).

$m = 1.0$, $n = 3.0$ sample after β→α-sialon transformation indicating that the amount of lithium and nitrogen in the grain boundary phase was more than that needed for β→α-sialon transformation, even though pure BN packing powder had been used. However, no new phase appeared in the $m = 0.5$, $n = 1.0$ and $m = 0.5$, $n = 2.0$ samples after heat treatment suggesting that the lithium in the grain boundary phase was totally consumed during β→α-sialon transformation when BN packing powder was used, whereas using Li-containing packing powder, the extra Li/N provided a further source for β→α-sialon transformation and thus more transformation occurred.

The very small amount of β–LiSiON(Al) observed after heat-treatment in these samples is believed to have crystallised from the grain boundary glass to balance the chemical composition at the heat-treatment temperature. A change also occurred in the chemical composition of α-sialon during heat-treatment as indicated by the changes in unit cell dimensions shown in Table 2. It was noticed that β→α transformation continued to proceed slowly but nevertheless convincingly with heat-treatment time in two-phase α/β samples as shown in Fig. 4. As can been from the figure, β→α transformation is slow because the transformation is reconstructive and can only be achieved by chemical reaction; moreover at such a low heat-treatment temperature (1200°C), the reaction requires a long time for completion. It was noted that the amount of transformation was more in the $m = 0.5$, $n = 2.0$ sample than in the others suggesting that there might be more grain boundary liquid in this sample; however, with further heat-treatment, transformation became very slow since most of the residual grain boundary liquid had been consumed after 168 h. Some β→α transformation occurred and the unit cell dimensions of α and the $z$-value of β changed a little.

### 3.1.2. Single-phase Li alpha sialons

In this case no α→β transformation occurred at all, and the only change on heat-treatment in BN packing powder was that the eucryptite disappeared, and β-LiSiON(Al) phase formed as shown in Table 1.

α-Sialon is still the predominant phase and no α→β transformation occurred even after heat-treatment for 336 h. However, the grain boundary phase changed and, for example, in $m = 1.0$ samples, the very small amount of eucryptite originally present disappeared and very weak β-LiSiON(Al) lines appeared after heat-treatment; in the case of the $m = 2$ series, although there was no α→β phase transformation, the XRD peaks of α became weaker and the peaks of both β-LiSiON(Al) and 21 R increased, suggesting that α-sialon was being converted into these phases, i.e.:

$$\alpha' \rightarrow 21\mathrm{R} + \beta - \mathrm{LiSiON(Al)} \quad (4)$$

Even though there was no α→β-sialon transformation, the unit cell dimensions of the α phase decreased after heat-treatment at 1200°C for 168 h indicating some adjustment in α-sialon composition. The changes in cell dimensions are given in Table 2 and the corresponding phase changes in Fig. 5.

## 3.2. Heat-treatment at 1300°C in BN packing powder

### 3.2.1. Two phase α/β-sialon samples

From the above discussion, it might be thought that α-sialon is more stable than β-sialon in the Li–Si–Al–O–N system at low temperature. However, because the α↔β-sialon transformation is reconstructive and temperatures such as 1200°C are very low for α↔β sialon transformation, it might be argued that the observed

β→α-transformation is not outside the bands of experimental error. Therefore, the same samples were heat treated at 1300°C for 168 and 500 h surrounded by BN packing powder to see if β→α-sialon transformation still occurred. The results are shown in Fig. 6 and Table 1.

It is clear that although the heat-treatment temperature is higher, the general transformation direction is the same, i.e. from β to α rather than the reverse and it was noticed that the amount of transformed β-sialon at 1300°C was nearly the same as that at 1200°C.

It has been reported previously that the unit cell dimensions of Ln and Y α-sialons change during low temperature heat treatment, always decreasing with time regardless of whether α→β sialon transformation occurs or

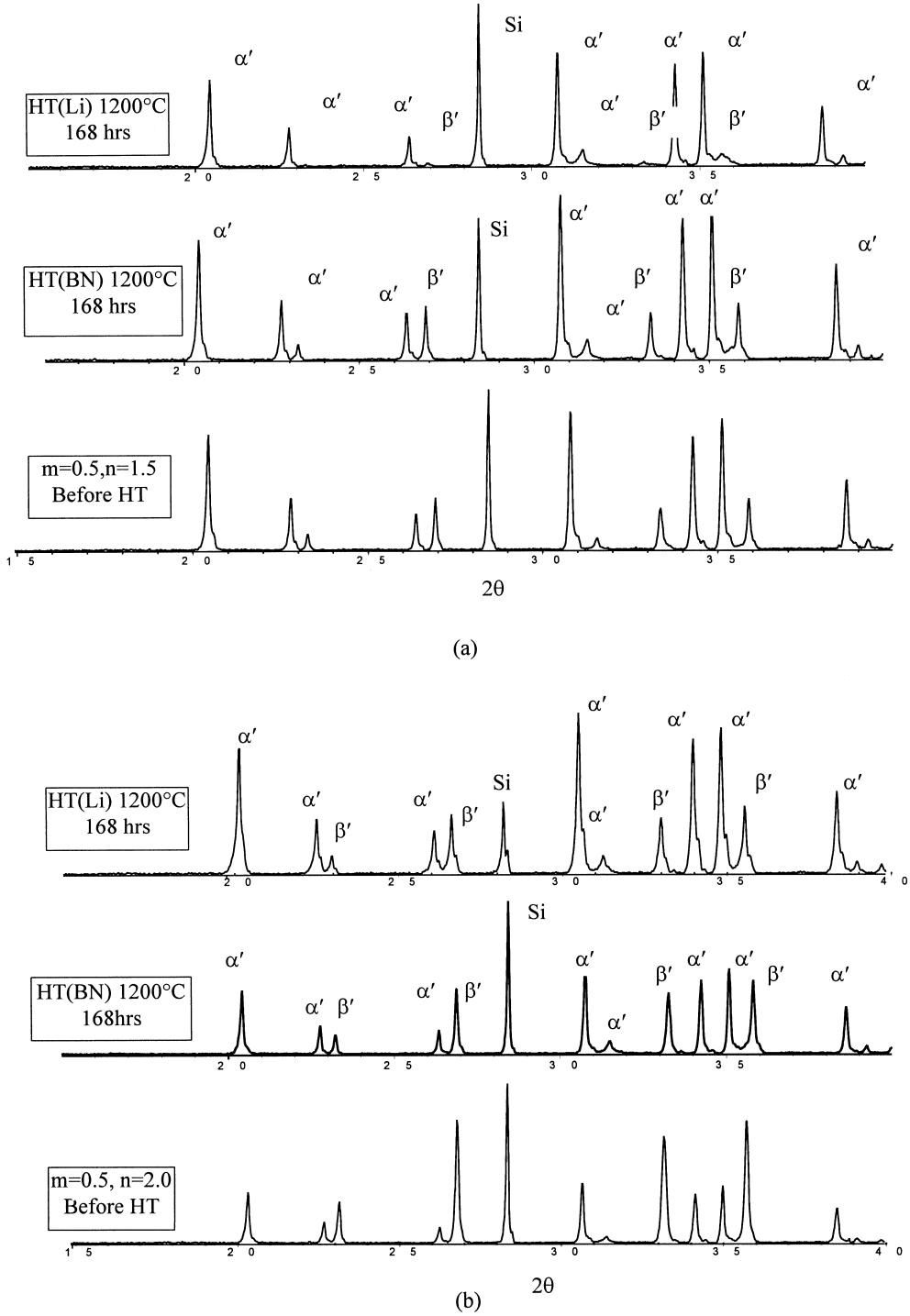


Fig. 2. XRD diffraction traces of (a) $m=0.5$, $n=1.5$ and (b) $m=0.5$, $n=2.0$ lithium two-phase α/β-sialon samples in the as-hot-pressed condition (HP) and after heat-treatment for 168 h at 1200°C surrounded by either BN- or lithium-containing packing powders.

not.[5,13,14,18,19] However, in the present study, as shown in Fig. 7, during β→α-sialon transformation in the $m=0.5$, $n=1.5$ and $m=0.5$, $n=2.0$ samples, the **a** unit cell dimension did not change very much; in the case of the $m=1.0$, $n=3.0$ sample, the **a** cell dimension decreased with increasing heat-treatment temperature, because in this sample, the original β-sialon content is lower and this can be easily totally converted into α-sialon after 168 h. When β→α-sialon transformation is complete, further increase in heat-treatment temperature or time will cause α→β-sialon transformation, but this time by a mechanism of Li volatilisation. The fact that $z$-values (Table 3) for the newly-formed β-sialons are nearly the same in the $m=1.0$, $n=3.0$ sample heat-treated at 1300 and 1450°C may further confirm this suggestion, which is discussed in more detail later.

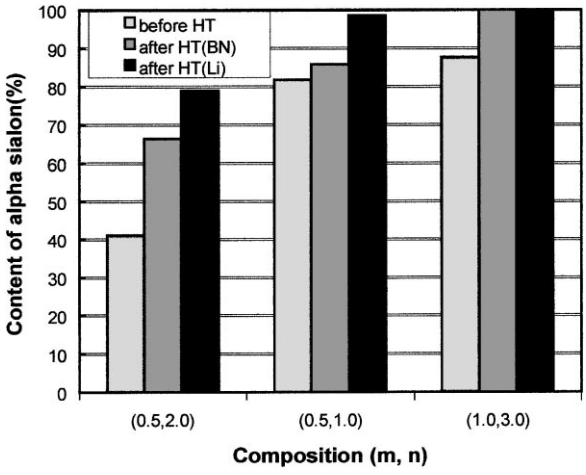


Fig. 3. Change in α-sialon content before and after heat-treatment at 1200°C for 168 h in different packing powders.

These results suggest that the β→α transformation in two-phase α/β-samples is actually a chemical reaction resulting in a new α composition forming, the reaction being:

$$\beta + \text{Li, N(from grain boundary liquid)} \rightarrow \alpha \quad (5)$$

### 3.2.2. Microstructural changes during transformation

As a result of β→α-sialon transformation, microstructures of samples changed during heat-treatment. Figs. 8 and 9 show typical SEM images of two-phase α/β-sialons of composition $m=0.5$, $n=2.0$ and $m=1.0$, $n=3.0$ before and after heat-treatment. Because in the Li–Si–Al–O–N system, α, β and glassy phases have almost the same average atomic number, the common method of using back-scattered electron images to distinguish α and β sialons, which relies on differences in mean atomic number, is not effective. Therefore, the microstructures shown here are secondary electron images. Samples were polished and etched with molten KOH to define the grain shape clearly.

Table 2
α-Sialon unit cell dimension changes before and after heat-treatment at low (1200–1450°C) temperatures

| Composition ($m$, $n$) | As HP | 1200°C/168 h (Li) | 1200°C/168 h (BN ) | 1200°C/336 h (BN) | 1300°C/168 h (BN) | 1300°C/500 h (BN) | 1450°C/168 h (BN) |
|---|---|---|---|---|---|---|---|
| | UCD (Å) | UCD (Å) | UCD (Å) | UCD (Å) | UCD (Å) | UCD (Å) | UCD (Å) |
| (0.5, 1.5) | 7.8011 | 7.8033 (4) | 7.8015 (4) | 7.8029 (3) | 7.8004 (6) | 7.7983 (5) | 7.8028 (5) |
| | 5.6691 | 5.5598 (4) | 5.6685 (4) | 5.6698 (4) | 5.6683 (4) | 5.6620 (5) | 5.6694 (8) |
| (0.5, 2.0) | 7.8055 | 7.8091 (5) | 7.8069 (4) | 7.8074 (5) | 7.8069 (5) | 7.8043 (5) | 7.8071 (4) |
| | 5.6853 | 5.6765 (5) | 5.6739 (4) | 5.6759 (5) | 5.6750 (4) | 5.6750 (5) | 5.6746 (4) |
| (1.0, 1.0) | 7.8131 | 7.8106 (6) | 7.8129 (5) | 7/8077 (3) | 7.8095 (3) | 7.8064 (4) | 7.8074 (5) |
| | 5.6677 | 5.6771 (5) | 5.6643 (5) | 5.6671 (3) | 5.6667 (2) | 5.6652 (4) | 5.6678 (4) |
| (1.0, 2.0) | 7.8245 | – | – | – | 7.8204 (5) | 78143 (4) | 7.8161 (4) |
| | 5.6780 | | | | 5.6821 (5) | 5.6834 (4) | 5.6836 (4) |
| (1.0, 2.5) | 7.8243 | 7.8225 (3) | 7.8237 (2) | 7.8243 (5) | 7.8215 (3) | 7.8180 (4) | 7.8219 (3) |
| | 5.6847 | 5.6811 (4) | 5.6829 (3) | 5.6832 (4) | 5.6878 (3) | 5.6857 (3) | 5.6818 (4) |
| (1.0, 3.0) | 7.8281 | 7.8257 (4) | 7.8262 (4) | 7.8261 (2) | 7.8270 (5) | 7.8192 (4) | 7.8247 (3) |
| | 5.6916 | 5.6869 (4) | 5.6887 (4) | 5.6905 (3) | 5.6883 (4) | 5.6879 (4) | 5.6878 (3) |
| (1.3, 1.2) | 7.8219 | – | – | – | – | – | 7.8214 (4) |
| | 5.6736 | | | | | | 5.6700 (4) |
| (1.5, 1.5) | 7.8308 | – | – | – | – | 7.8103 (5) | 7.8284 (4) |
| | 5.6821 | | | | | 5.6755 (5) | 5.6788 (4) |
| (2.0, 1.5) | 7.8271 | – | – | – | – | – | 7.8257 (3) |
| | 5.6759 | | | | | | 5.6756 (3) |
| (2.0, 2.0) | 7.8321 | 7.8332 (6) | 7.8318 (4) | 7.8335 (4) | 7.8319 (5) | 7.8189 (4) | 7.8298 (3) |
| | 5.6802 | 5.6769 (4) | 5.6776 (7) | 5.6774 (4) | 5.6773 (5) | 5.6811 (4) | 5.6809 (3) |
| (2.0, 2.5) | 7.8325 | 7.8334 (5) | 7.8295 (4) | 7.8327 (5) | 7.8308 (4) | 7.8127 (4) | 7.8303 (4) |
| | 5.6820 | 5.6798 (7) | 5.6790 (5) | 5.6803 (4) | 5.6837 (6) | 5.6806 (4) | 5.6816 (5) |
| (2.0, 3.0) | 7.8352 | 7.8342 (6) | 7.8320 (5) | 7.8308 (5) | 7.8327 (7) | 7.8260 (5) | 7.8304 (5) |
| | 5.6836 | 5.6772 (6) | 5.6813 (7) | 5.6806 (5) | 5.6849 (9) | 5.6868 (5) | 5.6871 (4) |

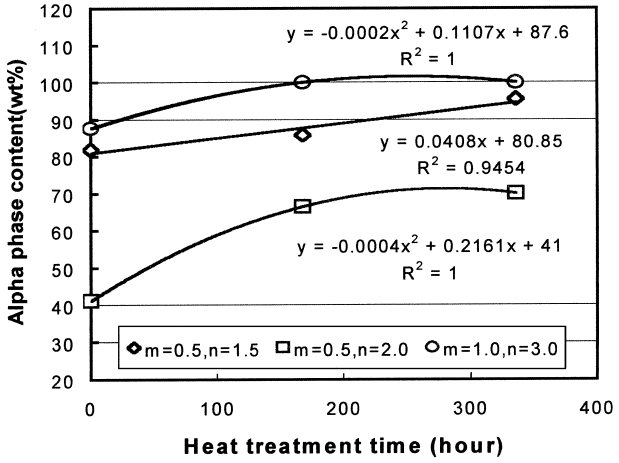


Fig. 4. Change in α-sialon content with heat-treatment time for mixed α/β samples heat-treated at 1200°C in BN packing powder.

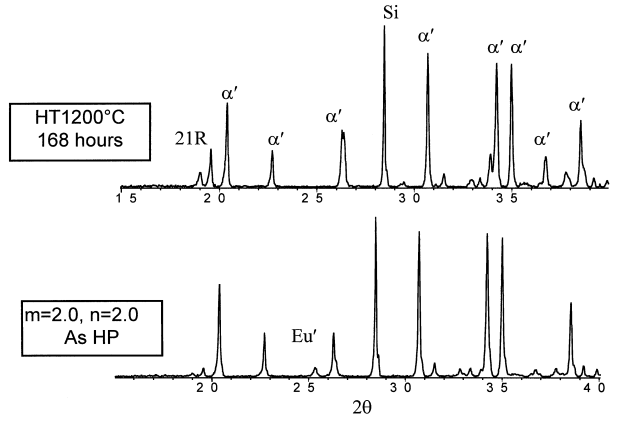


Fig. 5. Phase changes of α-sialon in the $m=2.0$, $n=2.0$ sample before and after heat-treatment at low temperature showing the disappearance of eucryptite.

Fig. 8 shows the microstructures of sample $m=0.5$, $n=2.0$ before and after heat-treatment. The sample contains both α and β phases with an α/β ratio of 41:59. Fig. 8(a) clearly shows that the microstructure consists of equiaxed α grains and elongated β grains with an aspect ratio of ≈10. The equiaxed α grains are very regular with diameters of about 1 μm and the β grains are well developed and have a perfect hexagonal section perpendicular to the growth direction. Since the starting composition was designed to produce pure α phase, and since there is 59% of β phase present, there must be some Li-containing liquid left in the grain boundary. This not only provides a suitable environment for the formation of the equiaxed α grains but also assists β growth by a solution–precipitation mechanism; therefore, the sample was relatively easily etched. After heat treatment at 1300°C for 168 h, the α/β ratio changed from 41:59 to 66:34 and the microstructure also changed significantly [see Fig. 8(b)]. Firstly, it was found that the sample was difficult to etch under the same etching conditions suggesting that there was less liquid in the sample because β→α transformation had consumed most of the liquid in the grain boundary. Secondly, it was noticed that most of the elongated β grains had disappeared, or rather had transformed into small α grains.

Fig. 9 shows the changes in the $m=1.0$, $n=3.0$ sample. In this sample, as discussed above, the α/β ratio was 87:13 before heat-treatment and, therefore, some elongated β grains could be found in the microstructure [Fig. 9(a)]; however, after heat-treatment, the α/β ratio was 100:0 and the β phase had been converted completely into α. The sample was, therefore, difficult to etch and it was difficult to discern any elongated β grains. These changes in both crystalline phase and microstructure contribute to an increased hardness after β→α transformation.

### 3.2.3. Pure alpha sialons

Pure α-sialons did not transform to β-sialon at 1200°C even after 336 h. The same samples were therefore heat treated at 1300°C for 168 h, but again no α→β transformation occurred. However, when the heat-treatment time was increased to 500 h at this temperature, α→β transformation did occur except for samples with $1<m<1.5$. Fig. 10 shows the XRD patterns of the sample $m=2.0$, $n=2.0$ before and after heat-treatment.

The phase changes and relative amounts of α and β phases after heat treatment are shown in Table 1 and Fig. 10. It is generally thought that pure α-sialon with a higher $m$ value should be more stable than samples with lower $m$ values; this idea is based on a transformation mechanism involving diffusion of metallic cations out of the α-sialon structure.[11] However, from the present study, this was not always observed to be the case.

As indicated in Fig. 11, not only does the $m$ value have a dominant effect on α→β transformation (as generally accepted), but the $n$ value also has an effect. The results indicate that for a given $n$ value pure Li-α-sialons with lower $m$ values are more stable than those with higher $m$ values. For instance, for pure α-sialons with $n=2.0$, when $m$ increased from 1.0 to 2.0, the content of transformed α increased from 2.2 wt% to 11.7 wt%; in the same way, pure Li–α-sialons with lower $n$ values are more stable than those with higher $n$ values for a given $m$ value. For example, for pure α-sialons with $m=2.0$, when $n$ increases from 2.0 to 2.5, the content of the transformed α increased from 11.7 wt% to 22.5 wt% after heat-treatment at 1300°C for 500 h.

Even though no α→β-sialon transformation was observed after 168 h of heat-treatment, the unit cell dimensions of α-sialon reduced a little, corresponding to a reduction in $m$ value. At this stage, the structure was still α, and hence was still in the single-phase region. However, when the heat-treatment time was prolonged to 500 h, α→β-sialon transformation occurred and the

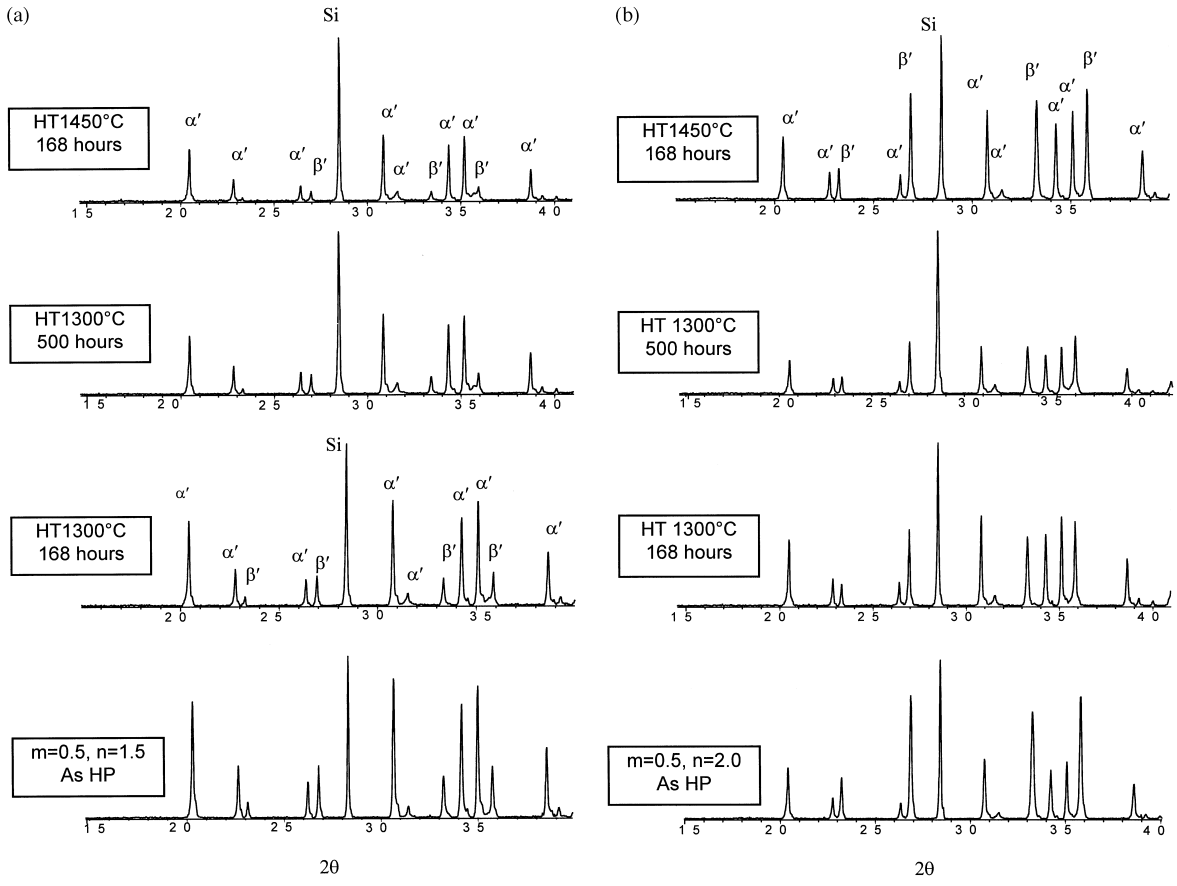


Fig. 6. XRD results of (a) the two phase α/β-sialon $m=0.5$, $n=1.5$ and (b) the two-phase α/β-sialon $m=0.5$, $n=2.0$ samples before and after heat-treatment in BN packing powder.

unit cell dimensions reduced significantly, especially for the $m=2.0$ series, changing to values very similar to α-sialons with $m=1.0$ (see Fig. 12). This showed that the compositions of the α-sialons with $m=2.0$ ($m_1$) moved across the single phase region ($m_2<2$) to the α/β two-phase region ($m_3<1$) after 500 h heat-treatment, where $m_1>m_2>m_3$.

### 3.3. Heat-treatment at 1450°C

#### 3.3.1. Two phase α/β-sialon samples

The heat treatment conditions of 1300°C for 168 h were still not sufficient to achieve complete α→β transformation. Samples were therefore further heat treated at 1450°C for 168 h in BN packing powder to see if more α→β transformation occurred. Under such heat-treatment conditions, it was thought that α→β transformation would occur, as previously observed with rare earth alpha sialons.

As shown in Fig. 6(a) and (b) and Table 1, despite the higher heat-treatment temperature, the general direction of transformation at 1450°C is still from β to α rather than the reverse. Whereas the amount of transformed β-sialon at 1300°C was about the same as that at 1200°C, at 1450°C it was noticeably less showing that the β→α-sialon transformation at these temperatures had been followed by some α→β-sialon transformation due to Li loss.

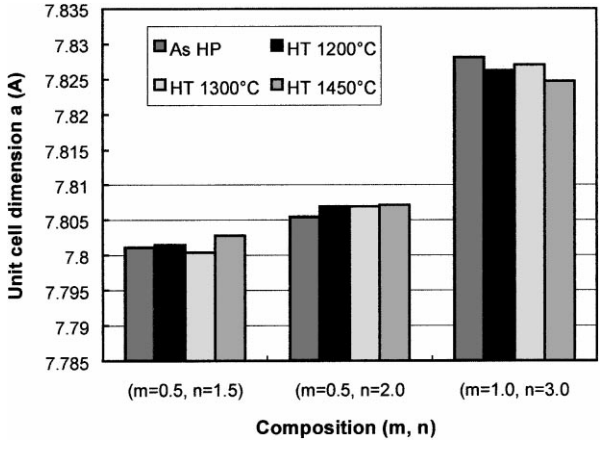


Fig. 7. The **a** unit cell dimension of α-sialon plotted vs heat-treatment temperature for samples heat-treated in BN packing powder for 168 h.

#### 3.3.2. Single-phase alpha sialons

None of these samples transformed to β after 168 h of heat-treatment at 1200°C and 1300°C. However, when the heat-treatment temperature was increased to 1450°C

for 168 h, α→β-sialon transformation occurred for compositions located on the boundary of the single phase region, except for the $m=1.0$, $n=1.0$ composition, which remained pure α.

It is interesting that although α→β transformation occurred in the $m=1.0$, $n=2.5$ sample, no other phases could be detected by XRD after transformation, and therefore the transformation can be expressed as:

$$\alpha_1 + \text{Liquid (1)} \rightarrow \alpha_2 + \beta + \text{Liquid (2)} \quad (6)$$

this decomposition reaction suggesting that the newly formed β-sialon has consumed Si, Al, O and N from the α-sialon but left the Li, which has moved into the grain boundaries or (more likely) been lost by volatilisation. Fig. 13 shows typical secondary election SEM images of the $m=1.0$, $n=2.0$ sample before and after heat-treatment at 1450°C for 168 h. From Fig. 13(a) it can be seen that before heat-treatment, the sample is essentially single-phase α-sialon, with a very small amount of residual grain-boundary phase, but the microstructure is inhomogeneous, with some elongated α-sialon grains. After heat-treatment at 1450°C, the microstructure became more homogeneous, but still with small pores in the sample [see Fig. 13(b)], suggesting that after α→β transformation, some liquid phase had formed in the sample.

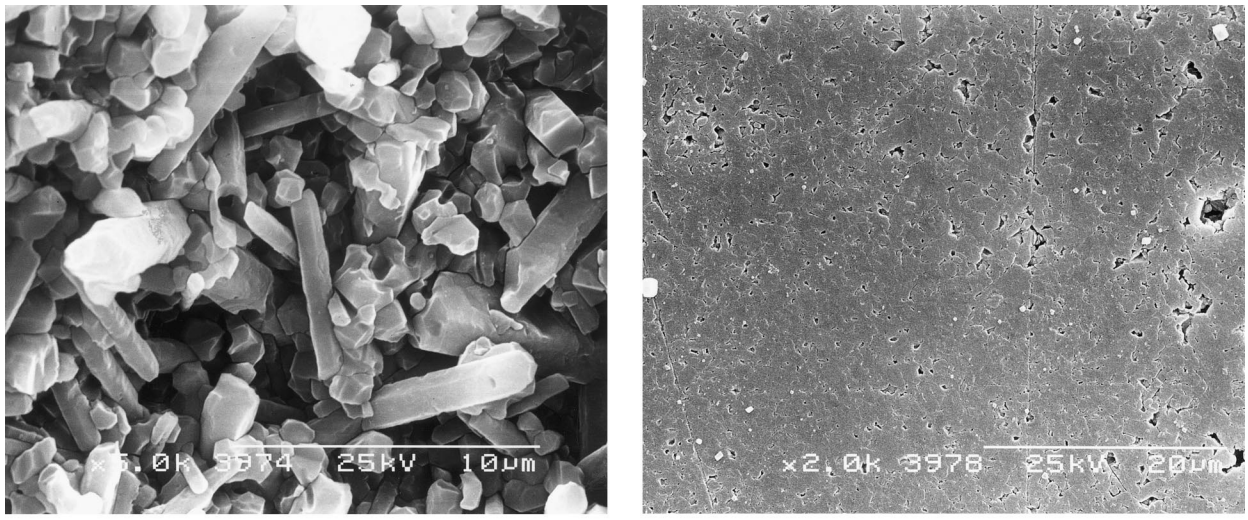


(a) (b)

Fig. 8. Microstructures of sample $m=0.5$, $n=2.0$ (a) before and (b) after heat-treatment at 1300°C for 168 h.

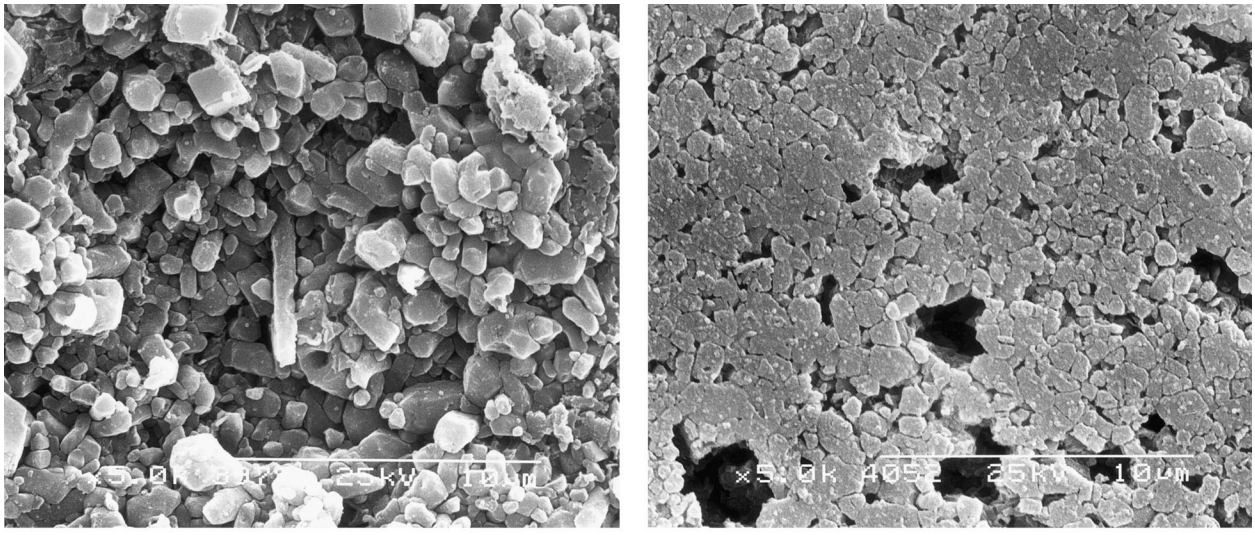


(a) (b)

Fig. 9. Microstructures of sample $m=1.0$, $n=3.0$ (a) before and (b) after heat-treatment at 1300°C for 168 h.

In the case of α-sialons with $m = 2.0$, new phases such as 15R and β-LiSiON(Al) were always present after heat-treatment (see Table 1). The transformation can be expressed as:

$$\alpha'_1 + 21\mathrm{R} + \mathrm{Eu.} \rightarrow \alpha'_2 + \beta' + 15\mathrm{R} + \beta - \mathrm{LiSiON(Al)} \quad (7)$$

Because the transformation products generally have a direct correlation with the transformation mechanism, it is believed that the transformation mechanism for α-sialons with low $m$ value is different from those of high $m$ value. The changes in unit cell dimensions are also different for α-sialons with different $m$ values as shown in Fig. 14.

Here, the changes in unit cell dimensions for α-sialons with high $m$ values are much smaller than those with low $m$ values after transformation even though the amount of transformed phase is nearly the same, suggesting that the compositions of α-sialons with high $m$ values did not change continuously with heat-treatment time and did not cross the single phase region during transformation. Therefore, it is believed that a direct decomposition mechanism, aided by grain-boundary liquid, is the predominant transformation mechanism in α-sialons with high $m$ values. Even though diffusion of

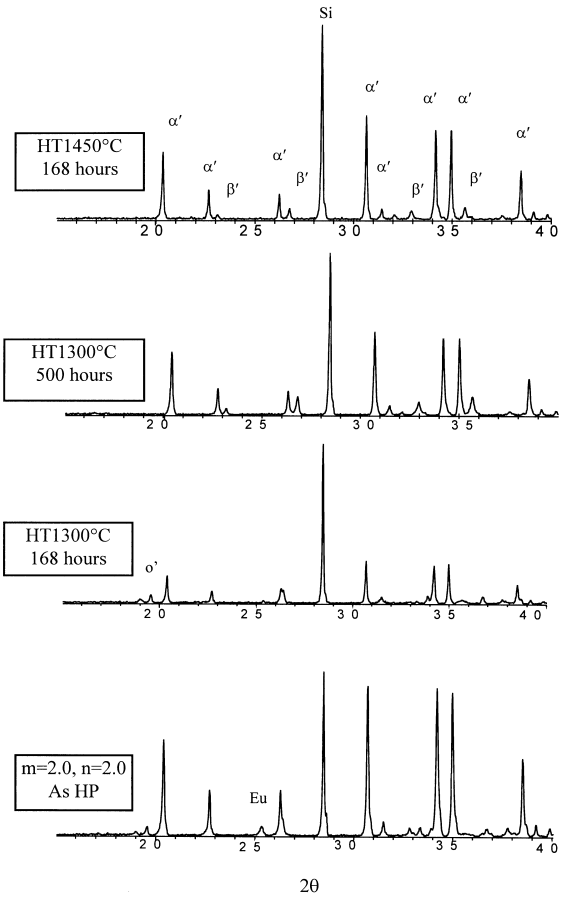


Fig. 10. X-ray patterns of the sample $m = 2.0$, $n = 2.0$ before and after heat-treatment in BK packing powder.

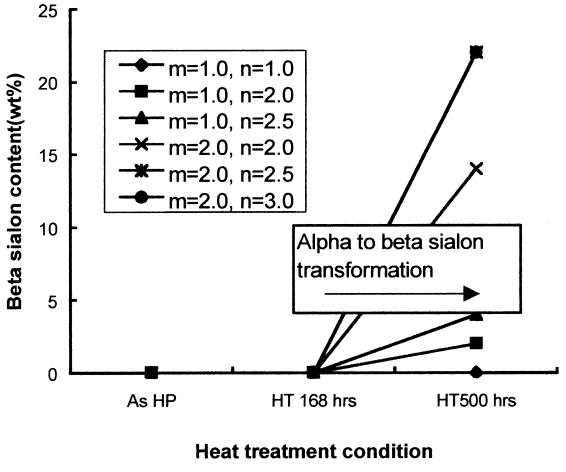


Fig. 11. Changes in β-sialon content with heat-treatment time for samples heat-treated at 1300°C in BN packing powder.

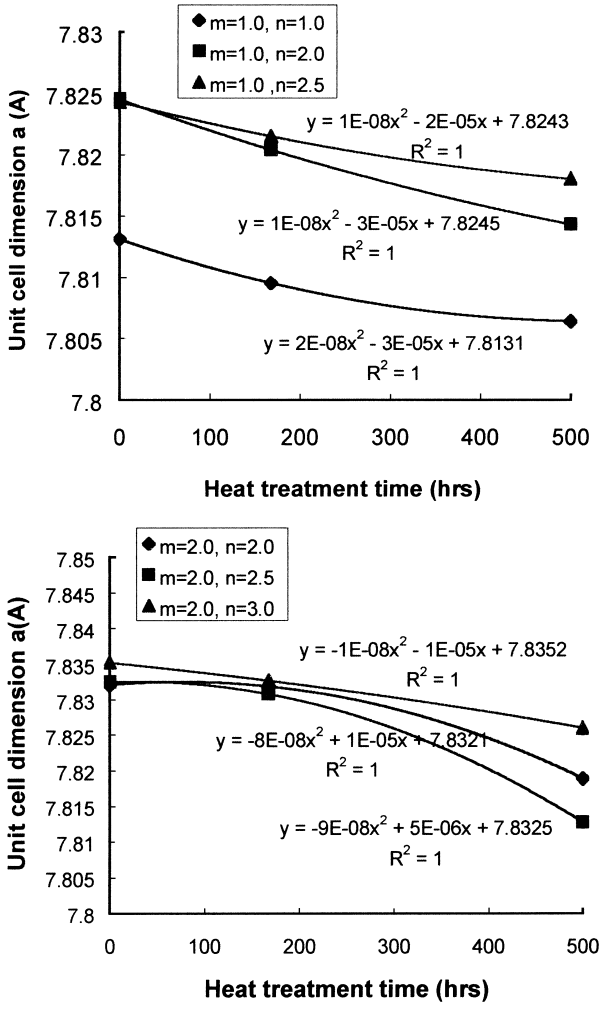


Fig. 12. Changes in **a** unit cell dimension of α-sialon with HT time.

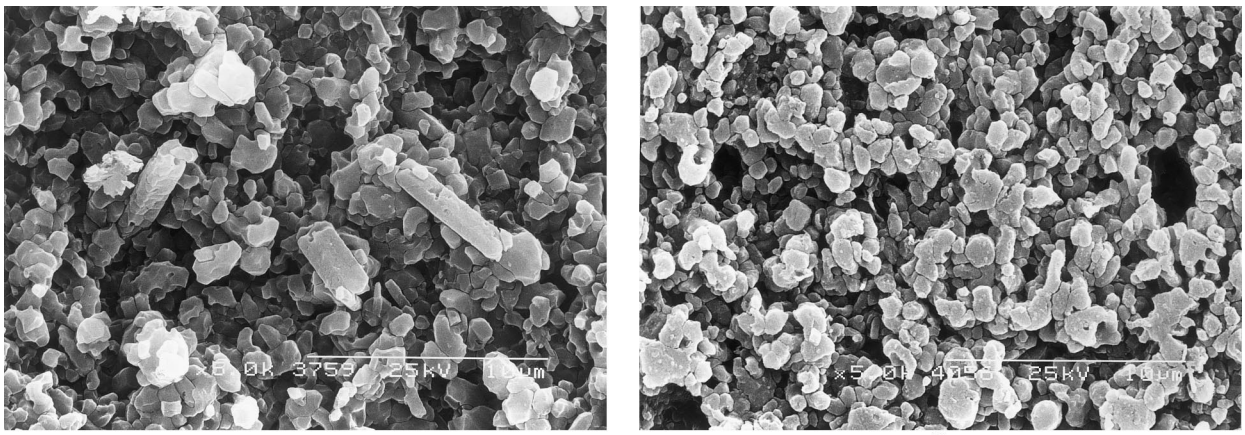


Fig. 13. SEM photographs of sample $m=1.0$, $n=2.0$, (a) before heat-treatment and (b) after heat-treatment.

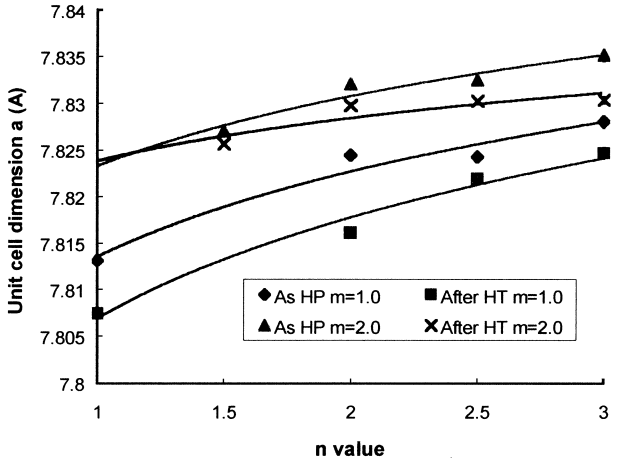


Fig. 14. a Unit cell dimension changes for various samples as a function of composition before and after heat-treatment at 1450°C in BN packing powder.

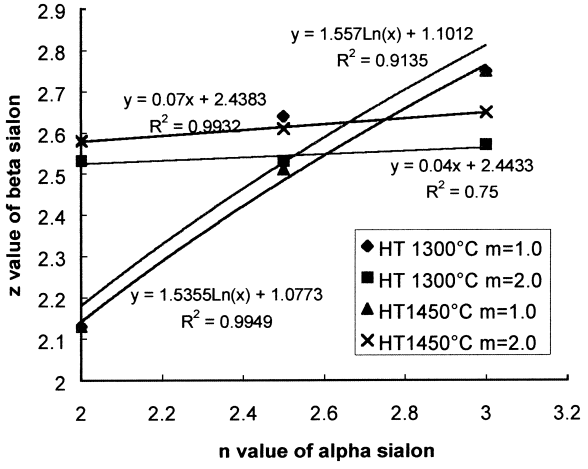


Fig. 15. Relationship between the $z$ value of β-sialon formed in α-sialons with different $m$ and $n$ values after heat-treatment in BN packing powder.

Li is involved in this process, the α unit cell dimensions did not change very much. The 15R AlN polytypoid phase was always present in the $m=2.0$ series (see Table 1). However, for α-sialons with low $m$ value, the cell dimensions changed significantly, in a similar way to those heat-treated at 1200 and 1300°C suggesting that diffusion of Li is the main transformation mechanism.

The $z$-value of the newly-formed β phase showed an interesting relationship with the original α-sialon composition as shown in Fig. 15. For $m=1$ compositions, the $z$ values increased significantly with $n$ value of the α-sialon starting composition and the relationship between $z$ value and $m$ and $n$ after heat-treatment at 1300°C is the same as that at 1450°C. However, different $m$ values resulted in a different $z$–$n$ relationship, namely: $z=(1.54\sim1.56)\ln(n)+1.10$ for $m=1.0$ compositions; and $z=(0.04\sim0.07)n+2.44$ (i.e almost independent of $n$) for $m=2.0$ compositions. The reason for the difference may be because the compositions of α-sialons changed in different ways. As shown in Fig. 1, on the Li–α-sialon plane, for α-sialons with low $m$ values, some Li and N have been lost by volatilisation or moved into grain boundaries during heat-treatment, which cause the transformed α-sialon composition to move towards the β-sialon line (i.e. $Si_3N_4$–$Al_3O_3N$ join) and thus $n$ has a strong effect on the $z$-value; however, for α-sialons with high $m$ values, Li and O have been lost by volatilisation or moved into grain boundaries, which make the newly-formed β-sialon compositions move towards the $Si_3N_4$ corner and therefore the original $n$ value has less effect on the newly formed β-sialon $z$ value.

## 4. Discussion

There is now a substantial body of literature on the phenomenon of $\alpha\Longleftrightarrow\beta$ sialon transformation, for α-sialons densified with Y or rare earth cations and prepared

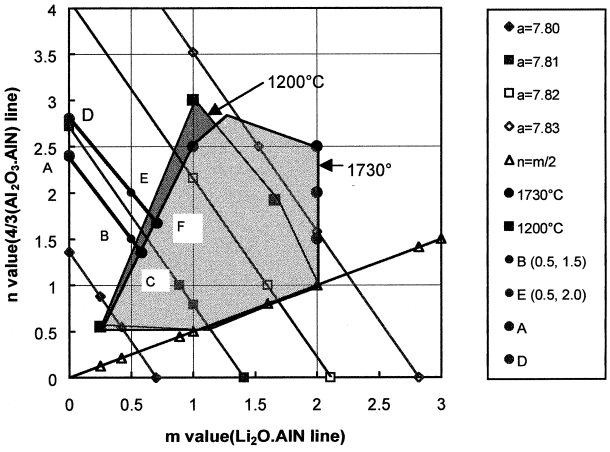


Fig. 16. Schmatic phase relationships in the α-sialon plane at high and low temperatures. As the temperature decreases, the single phase region shifts towards the β-sialon line.

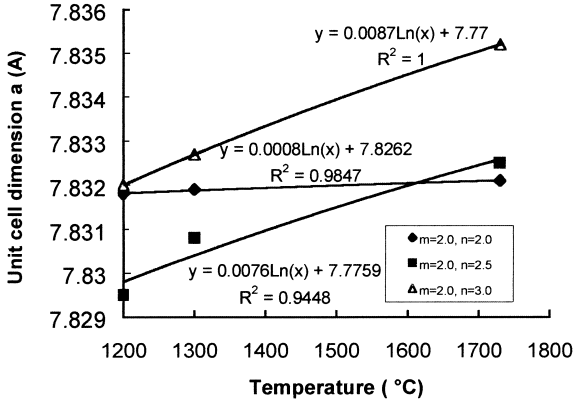


Fig. 17. Unit cell dimension of α-sialon ($m=2.0$) at different temperatures before $\alpha' \rightarrow \beta$ transformation.

at high (1700–1900°C) temperatures and then heat-treated at lower temperatures. However, this behaviour is not observed in the Li–α-sialon system and, as reported in our previous work,[20] the opposite transformation (i.e. $\beta \rightarrow \alpha$) occurs when two phase Li–α/β-sialon samples are heated at low temperatures.

This observation indicates that a chemical reaction is taking place of the type:

$$\alpha_1 + \beta_1 \xrightarrow[\text{Grain boundary liquid}]{} \alpha_2 + \beta_2 \quad (8)$$

where $\alpha_1$ represents a smaller amount of a higher Li α-sialon phase, $\alpha_2$ represents a larger amount of a lower Li α-sialon phase; $\beta_1$ and $\beta_2$ are β-sialon phases of similar $z$ value but with more $\beta_1$ present than $\beta_2$. An increased amount of nitrogen remains in the grain boundary phase(s). Because in the Li–Si–Al–O–N system, any heat-treatment temperature is higher than the eutectic temperature, some grain boundary liquid will be present and can assist β to α transformation. XRD analysis shows that very little crystalline grain boundary material remains in the sample, with no other phases except α and β being detected either before or after heat-treatment. The position of the α + β/α phase boundary can therefore be deduced by using the lever rule. So, the distance from the β-sialon line to the starting composition, divided by the total α–β distance gives the fraction of α present. Thus, if B stands for the starting $m=0.5$, $n=1.5$ composition, and E for the $m=0.5$, $n=2.0$ composition, and the compositions of α and β phases in these samples are represented by the points C, F and A, D respectively (see Fig. 16), then consideration of the phase analysis data in Table 1 shows that:

$$(BC)_{1700^\circ C} > (BC)_{1300^\circ C} \approx (BC)_{1200^\circ C}$$
$$(EF)_{1700^\circ C} > (EF)_{1300^\circ C} \approx (EF)_{1200^\circ C}$$

This suggests that the low $m$ limit of the single phase region systematically moves to lower $m$ values at low temperatures. This limit is not represented by a straight

Table 3
β-Sialon unit cell dimension changes after heat-treatment in BN [or Li-containing (L)] packing powders at low (1200–1450°C) temperatures

| Sample ($m$, $n$) | T (°C), T(h) | UCD (Å) | | $z$-Value |
|---|---|---|---|---|
| (0.5, 1.5) | As HP | 7.6437 | 2.9364 | 1.20 |
| | 1200°C, 168 h (L) | 7.6329 | 2.9382 | 1.05* |
| | 1200°C, 168 h | 7.6465 | 2.9369 | 1.25 |
| | 1200°C, 336 h | 7.6451 | 2.9380 | 1.25 |
| | 1300°C, 168 h | 7.6422 | 2.9371 | 1.20 |
| | 1300°C, 500 h | 7.6412 | 2.9370 | 1.17 |
| | 1450°C, 168 h | 7.6420 | 2.9380 | 1.20 |
| (0.5, 2.0) | As HP | 7.6508 | 2.9413 | 1.41 |
| | 1200°C. 168 h (L) | 7.6609 | 2.9382 | 1.25* |
| | 1200°C, 168 h | 7.6545 | 2.9441 | 1.52 |
| | 1200°C, 336 h | 7.6530 | 2.9458 | 1.55 |
| | 1300°C, 168 h | 7.6518 | 2.9452 | 1.50 |
| | 1300°C, 500 h | 7.6509 | 2.9541 | 1.48 |
| | 1450°C, 168 h | 7.6513 | 2.9455 | 1.51 |
| (1.0, 2.0) | As HP | – | – | – |
| | 1300°C, 500 h | 7.6743 | 2.9592 | 2.13 |
| | 1450°C, 168 h | 7.6744 | 2.9589 | 2.13 |
| (1.0, 2.5) | As HP | – | – | – |
| | 1300°C, 500 h | 7.6850 | 2.9765 | 2.64 |
| | 1450°C 168 h | 7.6840 | 2.9705 | 2.51 |
| (1.0, 3.0) | As HP | 7.6816 | 2.9632 | 2.32 |
| | 1300°C, 500 h | 7.6808 | 2.9863 | 2.75 |
| | 1450°C, 168 h | 7.6903 | 2.9782 | 2.75 |
| (2.0, 2.0) | As HP | – | – | – |
| | 1300°C, 500 h | 7.6810 | 2.9739 | 2.53 |
| | 1450°C, 168 h | 7.6850 | 2.9733 | 2.58 |
| (2.0, 2.5) | As HP | – | – | – |
| | 1300°C, 500 h | 7.6790 | 2.9761 | 2.53 |
| | 1450°C, 168 h | 7.6852 | 2.9795 | 2.61 |
| (2.0, 3.0) | As HP | – | – | – |
| | 1300°C, 500 h | 7.6823 | 2.9751 | 2.57 |
| | 1450°C, 168 h | 7.6865 | 2.9760 | 2.65 |

line parallel to the β-sialon line, but gets nearer to the latter with decreasing $n$ value and this case is true at both high and low temperatures.

In the same way, the high $m$ limit of the α phase region also systematically shifts to lower $m$ values at low temperature. As listed in Table 1, before any α→β transformation occurred, the XRD peaks of α became less strong and the peaks of both β-LiSiON(Al) and 21R polytypoid phase increased indicating that α-sialon decomposed and converted into these phases through the following equation:

$$\alpha \rightarrow 21R + \beta - LiSiON(Al) \quad (9)$$

This indicates that the amount of α-sialon in the sample is decreasing, i.e. the high $m$ limit of the α-sialon region moves towards the β-sialon line. The unit cell dimensions of α-sialon in the $m = 2.0$ series decreased with decreased temperature (see Fig. 17), also confirming that the compositions of $m = 2.0$ samples have moved to lower $m$ values after heat-treatment at low temperatures. Therefore, as illustrated in Fig. 16, at low temperatures, the whole single alpha phase region actually shifts towards lower $m$ values, i.e. towards the β-sialon line. This systematic shift is believed to explain the apparently abnormal β→α transformation behaviour observed in this system.

## 5. Conclusions

1. The range of Li–α-sialon stability varies with temperature shifting towards the β-sialon line at lower temperatures and vice versa.
2. In mixed α/β sialon compositions, a low Li content α-sialon phase is stable at low temperatures (< 1450°C), whereas at higher temperatures (> 1450°C) transforms to a smaller amount of a higher Li α-sialon phase with the appearance of more β. The transformation of the low Li α-sialon to high Li α-sialon plus β-sialon is in-situ via appropriate chemical reactions involving grain-boundary phase material.
3. Li-containing packing powder can facilitate β→α phase transformation by acting as an additional source of lithium.
4. Both heat-treatment temperature and time have effects on β→α phase transformation. The heat-treatment temperature should be higher than the eutectic temperature in the Li–Si–Al–O–N system (about 1050°C) to allow the liquid phase to assist in the process. Increasing temperature and time will facilitate the transformation below 1450°C. However, higher heat-treatment temperatures or increasing time will cause α→β phase transformation due to the volatilisition of Li from the α structure.
5. Single-phase Li α-sialons exhibit good thermal stability but this depends strongly on composition and the surrounding environment; α-sialons with compositions on the α/α+β boundary are less stable than those within the single phase region. The mechanism of α→β transformation is different at different temperatures and can be divided into two regimes. Firstly, single phase α-sialons continually adjust their compositions towards the α/α+β boundary during extended heat-treatment and this is followed by decomposition of the α phase; secondly, evaporation of the Li stabilising cation is the main reason for the transformation of α-sialons with low $m$ and $n$ values at higher temperatures. However, for α-sialons with high $m$ and $n$ values, self-decomposition is the process responsible for the α→β transformation at high temperatures.

## References


1. Hampshire, S. et al., α-Sialon ceramics. *Nature*, 1978, **274**, 880–882.
2. Cao, G. Z. and Metselaar, R., Alpha–sialon ceramics — a review. *Chemistry of Materials*, 1991, **3**, 242–252.
3. Mandal, H. et al., Mechanical property control of rare-earth–oxide densified alpha–beta sialon composites by alpha↔beta sialon transformation. In *5th International Symposium on Ceramic Materials and Components for Engines*, ed. D. S. Yan, X. R. Fu and S. X. Shi. World Science, Shang hai, China, 29 May–1 June 1994, pp. 441–445.
4. Thompson, D. P., α⟺β sialon transformation. In *Tailoring of Mechanical Properties of $Si_3N_4$ Ceramics*, ed. M. J. Hoffmann and G. Petzow. Kluwer Academic Publishers, The Netherlands, 1994, pp. 125–136.
5. Mandal, H., Thompson, D. P. and Ekström, T., Reversible α⟺β sialon transformation in heat-treated sialon ceramics. *J. Eur. Ceram. Soc.*, 1993, **12**, 421–429.
6. Shen, Z. J., Ekström, T. and Nygren, M., Reactions occurring in post heat-treated alpha/beta sialons — on the thermal-stability of alpha–sialon. *J. Eur. Ceram. Soc.*, 1996, **16**, 873–883.
7. Shen, Z. J., Ekström, T. and Nygren, M., Ytterbium–stabilized alpha–sialon ceramics. *J. Phys. D Applied Physics*, 1996, **29**, 893–904.
8. Shen, Z. J., Ekström, T. and Nygren, M., Temperature stability of samarium-doped alpha–sialon ceramics. *J. Eur. Ceram. Soc.*, 1996, **16**, 43–53.
9. Shen, Z. J., Ekström, T. and Nygren, M., Homogeneity region and thermal-stability of neodymium-doped alpha–sialon ceramics. *J. Am. Ceram. Soc.*, 1996, **79**, 721–732.
10. Shen, Z. J., Ekström, T. and Nygren, M., Preparation and properties of stable dysprosium-doped alpha–sialon ceramics. *J. Mat. Sci.*, 1997, **32**, 1325–1332.
11. Zhao, R. P. and Cheng, Y. B., Decomposition of sm alpha-sialon phases during postsintering heat-treatment. *J. Eur. Ceram. Soc.*, 1996, **16**, 1001–1008.
12. Zhao, R. P., Cheng, Y. B. and Drennan, J., Microstructural features of the alpha–sialon to beta–sialon phase-transformation. *J. Eur. Ceram. Soc.*, 1996, **16**, 529–534.
13. Hewett, C. et al., Calcium α-sialon ceramics. *Proc. of Mater. Res.*, 1996, **1**, 101–104.
14. Hewett, C. L. et al., The effect of glass additions on Ca α-/β-

SiAlON composites. Proc. of the 2nd Inter. Meeting of Pac. Rim Ceram. Soc., 1996.
15. Yu, Z. B., Thompson, D. P. and Bhatti, A. R., Preparation of single phase Li–α-sialon. *Brit. Ceram. Trans.*, 1998, **97**(2), 41–47.
16. Liddell, K., X-ray analysis of nitrogen ceramics, in Department of Mechanical, Materials, and Manufacturing Engineering. 1979, University of Newcastle upon Tyne.
17. JCPDS card, No. 34-963.
18. Camuscu, N., Thompson, D. P. and Mandal, H., Effect of starting composition, type of rare earth sintering additive and amount of liquid phase on alpha reversible arrow beta sialon transformation. *J. Eur. Ceram. Soc.*, 1997, **17**, 599–613.
19. Hewett, C. L. et al., Thermal stability of calcium α-sialon ceramics. *J. Eur. Ceram. Soc.*, 1998, **18**, 417–427.
20. Yu, Z. B., Thompson, D. P. and Bhatti, A. R., α⟺β-sialon transformation in Li-sialon ceramics. International Symposium on Nitrides II, Trans. Tech. Publications, Zurich, Switzerland, 9–11 June, University of Limerick, Ireland, 1998.